

Dynamic Modeling and Simulation of Natrium Energy Island with Molten Salt Energy Storage

Seth J. Dana¹, Aiden S. Meek¹, Jacob A. Bryan¹, Manjur R. Basnet¹, and Hailei Wang¹

¹Utah State University College of Engineering

March 23, 2024

Abstract

The increasing installment of solar and wind renewable energy systems create a volatile energy demand to be met by electricity providers. A nuclear hybrid energy system is a nuclear reactor with energy storage that integrates into the grid with renewable energy sources. The Natrium design by TerraPower and GE Hitachi is a sodium fast reactor with molten salt energy storage. The Natrium design operates at steady state of 345 MW_e and can boost up to 500 MW_e for 5.5 hours. This study uses Dymola and the Modelica language to model the Natrium-based NHES. The dynamic system model is tested using hourly historical data from Texas (ERCOT) 2021 to show how renewables affect the electricity demand and how energy storage affects the Natrium system response to the demand. According to the results, while the available storage will allow the Natrium design to boost electricity production when the demand and electricity price is high making it more economically viable, the current molten salt storage is undersized for the ERCOT market.

RESEARCH ARTICLE

Dynamic Modeling and Simulation of Natrium Energy Island with Molten Salt Energy Storage

Seth J. Dana | Aiden S. Meek | Jacob A. Bryan | Manjur R. Basnet | Hailei Wang

¹Department of Mechanical and Aerospace Engineering, Utah State University, UT, USA

Correspondence

Corresponding author Seth J. Dana
Email: sethjdana@gmail.com

Abstract

The increasing installment of solar and wind renewable energy systems create a volatile energy demand to be met by electricity providers. A nuclear hybrid energy system is a nuclear reactor with energy storage that integrates into the grid with renewable energy sources. The Natrium design by TerraPower and GE Hitachi is a sodium fast reactor with molten salt energy storage. The Natrium design operates at steady state of 345 MW_e and can boost up to 500 MW_e for 5.5 hours. This study uses Dymola and the Modelica language to model the Natrium-based NHES. The dynamic system model is tested using hourly historical data from Texas (ERCOT) 2021 to show how renewables affect the electricity demand and how energy storage affects the Natrium system response to the demand. According to the results, while the available storage will allow the Natrium design to boost electricity production when the demand and electricity price is high making it more economically viable, the current molten salt storage is undersized for the ERCOT market.

KEY WORDS

Natrium, NHES, IES, Modelica, Dymola, TES

Highlights

- A computationally efficient Dymola/Modelica model is developed to simulate potential deployment scenarios of the Natrium design.
- Dynamic simulation is performed in Texas (ERCOT) deregulated market. Renewables are removed from the demand profile to show increased volatility.
- The modified Rankine cycle coupled with a sodium-cooled fast reactor demonstrates a thermal efficiency of 42%, surpassing light-water reactors.
- The dynamic model takes ambient temperature and humidity as inputs, accurately predicting the corresponding trends.
- The simulation indicates the current Natrium design could benefit from a larger energy storage for ERCOT to meet the peaks in demand.

1 | INTRODUCTION

Climate change is an ever-present threat to our planet and its inhabitants. The consequences of global warming, including rising sea levels, extreme weather events, and food and water scarcity, are already being felt worldwide. To mitigate these impacts, many countries are transitioning away from fossil fuels and towards renewable energy sources to generate electricity without emitting greenhouse gases. One promising renewable energy technology is photovoltaic (PV) solar panels. Recent years there have been a significant reduction in the cost of PV solar panels, making them a more accessible and attractive option for electricity generation¹. This has resulted in a surge in their deployment globally, from 0.26 GW in 2000 to 16.1 GW in 2010, according to a study by Branker et al.¹. However, the use of renewables, like PV solar panels, pose new challenges to power

providers who must deal with a fluctuating energy demand that is not always met by these renewable sources². In such cases, conventional coal or gas power plants are used to meet the remaining fluctuating demand.

While renewables are promising, nuclear power remains an attractive alternative to fossil fuels. Traditional nuclear power plants have been primarily used for base load electricity generation, and their operation may not be well-suited for fluctuating loads. While the technology for load following nuclear power plants is available, the limiting factor preventing nuclear plants from load following is the economics due to a reduction in capacity factor³. The majority of the cost of a nuclear power plant is the upfront capital cost while the operating and fuel costs are relatively low compared to this capital expense⁴. This 'front-loaded' cost structure and low fuel cost (10-15% of electricity generation cost⁵) make constant base load power scenarios attractive for nuclear power⁴. In the case of fossil fuels, the operating costs dominate. Fuel costs of fossil fuels account for 70-80% of the electricity generation cost⁵.

Electric load following with the reactor alone requires modifying reactivity in the core by moving control rods in/out of the core. Reducing reactivity in the core wastes potential energy of the fuel and can cause thermal strain on the nuclear system⁶. Co-generation and thermal energy storage (TES) are two ways for nuclear power to load follow without the need to modify reactivity in the core⁷. Co-generation involves the production of electricity and another valuable product using energy from a single nuclear source. This other valuable product can be clean water through desalination, hydrogen production, or energy storage⁸. When the demand for electricity is high the plant will produce more electricity and when it is low the secondary product will be produced. This allows a nuclear plant to match with a variable electricity load while operating at a steady state on the nuclear side. This paper will focus on TES coupled with nuclear reactors to allow load following.

Recently, Mikkelsen et al.⁹ concluded that a control system can be established allowing near-constant operation of a nuclear reactor core at full power while following variable electrical load using a concrete TES. Their model allowed for electrical energy outputs between 70-120% of nominal power. The model was developed in Modelica language and included a detailed turbine model which allowed stage analysis. Esteves et al.¹⁰ assessed load following performance of a nuclear renewable hybrid energy systems (N-RHES) for fast-charging EV stations. Their model included hydrogen production and storage which would be converted back to electricity using a fuel cell during times of high demand or the hydrogen could be used for hydrogen fueled vehicles. Matlab/Simulink was used to model reactor core dynamics with steam generator dynamics due to its non-linear nature. Bryan et al.¹¹ studied the deployment of a N-RHES with two tank molten salt TES and hydrogen production and storage in Texas. They concluded that the system could produce large amounts of hydrogen during off peak times mainly in the spring and fall. They also concluded that the hydrogen fuel cell used to meet peak demands in the summer had a capacity factor of 3.1% and did not meet economic goals of the study. Garcia et al.¹² evaluated the value of N-HRES with wind, solar, and battery storage. The models were developed using Modelica. They concluded that N-HRES can operate in scenarios with high variable energy resources (renewables). Wodrich et al.¹³ developed a model in Modelica language to investigate deployment scenarios for micro-reactors in an energy diverse grid on a university campus. They concluded that using a micro-reactor solely to produce electricity would have the greatest impact on emission reduction. While dynamic operation using molten salt energy storage benefited by having a lower dependence on grid connection but showed lower emissions reduction and cost savings. Binder et al.¹⁴ modeled a nuclear, wind, and chemical plant hybrid energy systems (HES). They concluded that Modelica could be effectively used to model large complex systems with dynamic conditions and added significant advantage to evaluating control algorithms.

In this study, a computationally efficient Dymola/Modelica model is developed to simulate potential deployment scenarios of the Natrium design by GE Hitachi and TerraPower for various de-regulated energy markets in the US. Specifically, the Electric Reliability Council of Texas (ERCOT) is used in the case study. The model uses hourly data and can run multi-year simulations in several minutes. The following sections of this paper will discuss the Natrium system, the Modelica model and its key components, and a case study to demonstrate model capabilities.

1.1 | Natrium Design

The transition towards clean energy sources has brought the need for new nuclear technologies that can manage the volatility of renewable energy systems. Nuclear hybrid energy systems (NHES) are a potential solution that integrate nuclear power with renewables and energy storage. In time with the growing importance of NHES designs, the Natrium design by TerraPower and GE Hitachi provides an innovative solution.

The Natrium design includes a sodium fast reactor coupled with a two tank molten salt TES system, which can provide energy during periods of high demand or when renewable energy sources are not available. It is designed to physically separate the energy storage and conversion systems (the Energy Island) from the reactor system (the Nuclear Island). The heat from the

Nuclear Island is directly transferred to the TES which discharges that heat to the energy conversion system, or balance of plant (BOP), to produce electricity¹⁵. Specifically, the Natrium design has a Rankine cycle that converts the thermal energy from the TES into electricity. To better understand the performance of the Natrium Energy Island and perform various system simulations, this paper presents a dynamic model of the system using the Modelica language in Dymola.

One of the key advantages of the molten salt energy storage system is its ability to allow the Natrium reactor to operate at a fixed heat output, while the electricity production can vary according to the changing energy demand. This flexibility is essential in managing the volatility of renewable energy sources and meeting the varying energy demands of different regions.

The system includes a model based control scheme that follows a given demand profile, allowing the Natrium Energy Island to respond to changes in energy demand in real-time. Furthermore, the study performed a twenty day simulation that demonstrates the controls and response of the system, showing how the Natrium Energy Island can operate efficiently in different scenarios.

Overall, this study sheds light on the potential of the Natrium Energy Island as a reliable and efficient solution for managing energy demand in the context of growing renewable energy. The Energy Island model incorporates multiple turbine stages, feedwater preheaters and a reheater. Additionally, it considers ambient air temperature which can have a significant impact on cycle efficiency and operation. The optimization of TES capacity plays a large role in the economic success of the deployment of the Natrium system. The objective of this model is to verify component sizing and study deployment scenarios of the Natrium system for various energy markets. The dynamic model and case study provide valuable insights into the operation of the Natrium system in a volatile energy market.

2 | SYSTEM MODELING AND CONTROL

The model leverages some components from US Department of Energy Idaho National Laboratory's HYBRID library¹⁶ and Oakridge National Laboratory's TRANSFORM library¹⁷. Modelica is a modern equation based object oriented modeling language for differential algebraic equation (DAE) based physical modeling. Even the most complex physical systems can be composed of elementary components. Each component can be defined by governing laws of physics. Components in Modelica are interfaced through special nodes called connectors which communicate with other components in the model¹⁸. This concept allows for acausal modeling in which the user does not need to define input-output relations for the variables. Commercial Modelica software environments, like Dymola¹⁹, come with advanced compiler and implicit solvers that can manipulate and solve the DAE system allowing the modeler to focus on physical modeling rather than algorithm selection and mathematical formulation¹⁸.

2.1 | System Parameters and Assumptions

This section will examine the assumptions and components that are incorporated into the model. The model does not intend to incorporate nuclear kinetics of the sodium fast reactor in the Energy Island; instead, it employs a simplified heat addition that simulates the constant heat input equivalent to the reactor. The molten salt will act as a coolant as it is pumped through the reactor model. The baseline electricity output of the model is set at 345 MWe, with the capability to increase to 500 MWe for a duration of 5.5 hours²⁰. Table C2 illustrates the primary input parameters utilized in the Dymola model.

The system operates between power levels of 200-500 MWe. This allows the system to store heat in the hot tank when operating below 345 MWe. Given the system is modeled in an hour interval, the transient/dynamic behavior within an hour is not modeled. This assumes all components in the system has reasonable time constant less than 20 minutes. Thus, the system is assumed always under quasi steady state during the simulation. The steam turbines have a fixed isentropic efficiency of 87%.

The Modelica model consists of three parts: sodium fast reactor, molten salt TES, and Rankine power cycle. Figure 1 shows a schematic of the system from Dymola.

2.2 | Sodium Fast Reactor

The sodium fast reactor model is simplified down to a constant heat rate added to the molten salt storage. Heat is added to the molten salt storage through a volume component with a constant heat rate. The mass flow rate through the reactor is determined by,

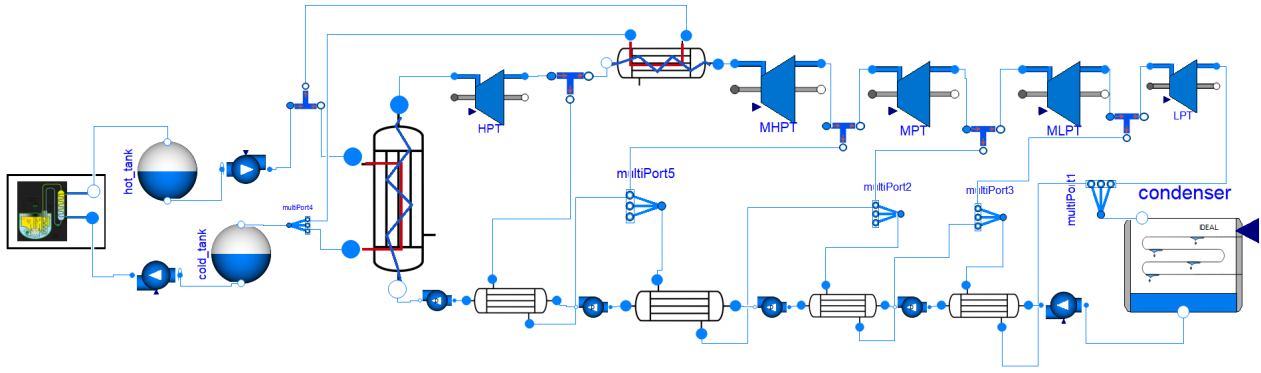


FIGURE 1 Schematic of the Dymola model.

$$Q_{in} = \dot{m}_{salt} c_{p,salt} (T_{hot} - T_{cold}) \quad (1)$$

where

$$Q_{in} = \frac{P_{baseload}}{\eta_{thermal}} \quad (2)$$

and $P_{baseload} = 345$ MWe. The flow rate of molten salt through the reactor will remain constant during simulations. Thus, this section of the model is referred to as the Nuclear Island model, while the remaining portions of the model are called the Energy Island model.

2.3 | Molten Salt TES

The energy storage system is comprised of two molten salt storage tanks, a hot and cold tank, and two pumps. The hot tank is used to store thermal energy from the sodium fast reactor and directly provide energy to drive the steam cycle. Afterwards, it returns to the cold tank. The lower-temperature salt coming out of the cold tank is circulated back into the reactor to absorb thermal energy. The mass flow rate from the cold tank to the hot tank (through the reactor) remains a constant while the flow rate from the hot tank to the cold tank (through the steam generator) varies with the energy demand.

The amount of energy in the Salt tanks is governed by

$$\frac{dU}{dt} = \dot{m}_{in} h_{in} - \dot{m}_{out} h_{out} \quad (3)$$

The TES allows the system to dynamically follow a load profile while the nuclear reactor can operate at steady state. The TES is modeled in Dymola using tank and pump models from the TRANSFORM library. The pumps are controlled by mass flow rate.

The medium in the TES uses molten nitrite salt also called Solar Salt. Its composition is 60% NaNO_3 and 40% KNO_3 . The properties of solar salt are shown in Table B1. Solar salt has been used in concentrated solar power for sensible heat storage due to its thermal stability at high temperature, desirable heat transfer properties at high temperatures up to 600°C , low vapor pressure and viscosity, non-toxicity, and non-flammability²¹. One limitation of solar salt is its high melting temperature of 220°C which means the operating temperature in the cold tank needs to be above 290°C with a reasonable margin.

The solar salt tanks hold 852.5 MWh of electrical storage which allows the Rankine cycle to boost power output from 345 MW_e to 500 MW_e for 5.5 hours.

2.4 | Reheat Rankine Cycle with Regeneration

Electricity is generated from a Rankine reheat cycle with one reheat stage and four feedwater preheaters (also called regenerators). The preheaters use steam bled from the turbines to heat pressurized water leaving the condenser before it enters the steam generator. Figure C3 and C4 shows the T-s diagram and state points diagram respectively for the Rankine cycle with feedwater preheating and a steam reheat after the first stage.

A steady state model developed in python is used to determine the optimal pressures, turbine bleed ratios, and feedwater preheat temperature stages²². When the turbine is operating at a power level less than the maximum (500 MWe) the flow rate is reduced by partial arc administration, a feature in the turbine model¹⁷. The steady state python model also provides the initial pressures and temperatures at all of the state points in the dynamic model, as well as the nominal flow rates necessary for the controller. Genetic algorithm was used to determine the optimal values of the state points in the steady state model. The steady state model sets the nominal mass flow rate for power output of 500 MW_e.

The steady state python model determines optimal values for the steam cycle parameters by using a genetic algorithm and provides them as inputs for the Dymola model. The steady state model set to run at an output of 500 MWe. The corresponding nominal flow rate provided is scaled down in the Dymola controller for different power outputs.

2.4.1 | Turbine

The turbine models are leveraged from the TRANSFORM Library developed by the Oakridge National Lab. They expand high pressure steam to a lower pressure to gain mechanical power. The following equations calculate the power produced by each turbine.

$$\dot{W} = \eta_{mech} \dot{m} (h_{in} - h_{out}) \quad (4)$$

In the model, the mechanical efficiency of the turbine is assumed to be 1.0, while the isentropic efficiency is equal to 0.87. The isentropic efficiency is used to calculate the outlet enthalpy of the turbine.

$$h_{in} - h_{out} = \eta_{is} (h_{in} - h_{is}) \quad (5)$$

The turbine is operated at power levels between 200-500 MW_e. The partial arc administration ($Arc_{partial}$) in the turbine model is used to calculate the outlet pressure of the turbine as shown in the following equation. The model is configured such that the outlet pressure of the turbine will remain the same for all power levels of the turbine. This is done by scaling the partial arc variable proportionally with the mass flow rate.

$$\dot{m} = \frac{P_{out} Arc_{partial} \dot{m}_{nom}}{P_{in,nom}} \quad (6)$$

The model uses 5 turbine models to allow for steam bleeding during steam expansion. The quality of the steam is 1.0 in all turbines except for the low pressure turbine (LPT) where it is 0.91. Thus, the Baumann factor was not considered in the turbine model.

2.4.2 | Heat Exchangers

The Model contains several heat exchangers including the steam generator, reheater, and feedwater preheaters (regenerators). Most of these heat exchangers involve phase change. Boiling happens in the steam generator while condensation happens on the vapor side of the preheaters. While some of the heat exchanger models available in the open source libraries provide detailed geometry and temperature profiles they are typically computationally expensive for large system modeling, especially when the fluid experiences phase change. Since the scope of this model is a computationally inexpensive simulation without the need for exact design parameters and heat exchanger geometry, the heat exchangers in this model use an effectiveness and energy balance to determine the outlet temperatures.

The heat exchangers in the model use a modified effectiveness (ϵ) equation. Each heat exchanger has a defined effectiveness which is used to calculate the outlet states,

$$h_{out,1} = h_{in,1} - \frac{\epsilon (\mathbf{min}(\Delta h_{Max}))}{\dot{m}_1} \quad (7)$$

ϵ is the effectiveness of the heat exchanger (given), \dot{m}_1 is the mass flow rate, and $\mathbf{min}(\Delta h_{(Max)})$ is the minimum of the maximum enthalpy differences possible in the heat exchanger,

$$\Delta h_{Max} = \left[\begin{array}{l} \dot{m}_1 (\mathbf{h}(T_{1,in}, P_1, X_{1,in}) - \mathbf{h}(T_{2,in}, P_1)), \\ \dot{m}_2 (\mathbf{h}(T_{2,in}, P_2, X_{2,in}) - \mathbf{h}(T_{1,in}, P_2)) \end{array} \right]. \quad (8)$$

Equations 7 and 8 are in terms of enthalpy change, instead of temperature, because of the phase change that happens in the heat exchanger. This method does not guarantee the second law of thermodynamics is followed, however, the pinch points were checked and validated to meet the requirements of the second law. In the regenerators, to ensure the second law of thermodynamics is satisfied, the outlet temperature of the feedwater is required to be 5 °C below the saturation temperature of the steam. Figure 2 shows how the second law of thermodynamics is satisfied in all four regenerators. As shown, there is a gap between the feedwater outlet temperature and the steam saturation temperature. After the four regenerator stages, the feedwater receives almost 350 MW as shown in the x-axis. The pinch points are also checked for the steam generator and reheater shown in the Appendix.

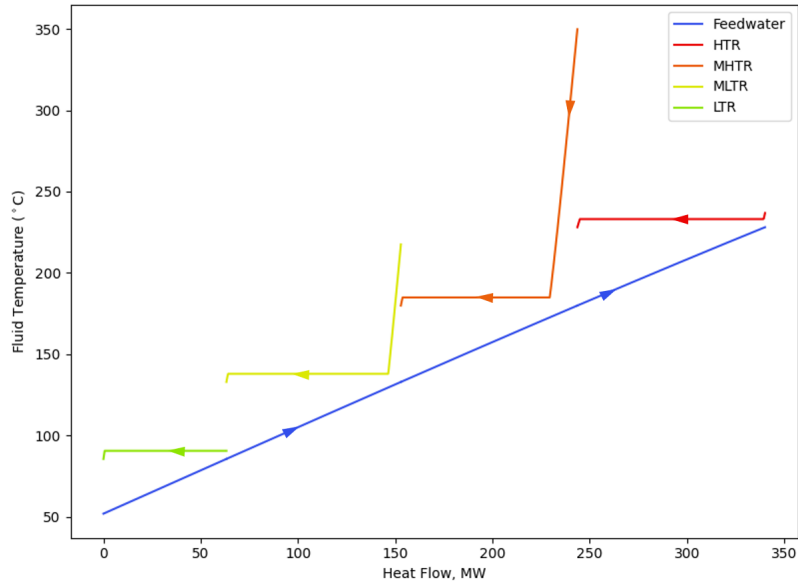


FIGURE 2 Temperature profiles within regenerators.

2.4.3 | Condenser

The condenser model allows the condensing pressure to change with the ambient wet bulb temperature in order to better reflect its actual operation. The condensing pressure is determined by

$$P_{cond} = \text{saturationP_T}(T_{wet} + 20^{\circ}\text{C}). \quad (9)$$

where **saturationP_T** is a function that returns the saturation pressure given a temperature. The condensing pressure is 20 C above the wet bulb temperature to provide reasonable temperature gradient in the condenser and account for the non-ideal performance in the cooling tower.

The varying condensing pressure has an effect on the thermal efficiency of the system. The higher the ambient wet bulb temperature, the lower the thermal efficiency due to the higher saturation pressure as temperature increases.

2.5 | Control Scheme

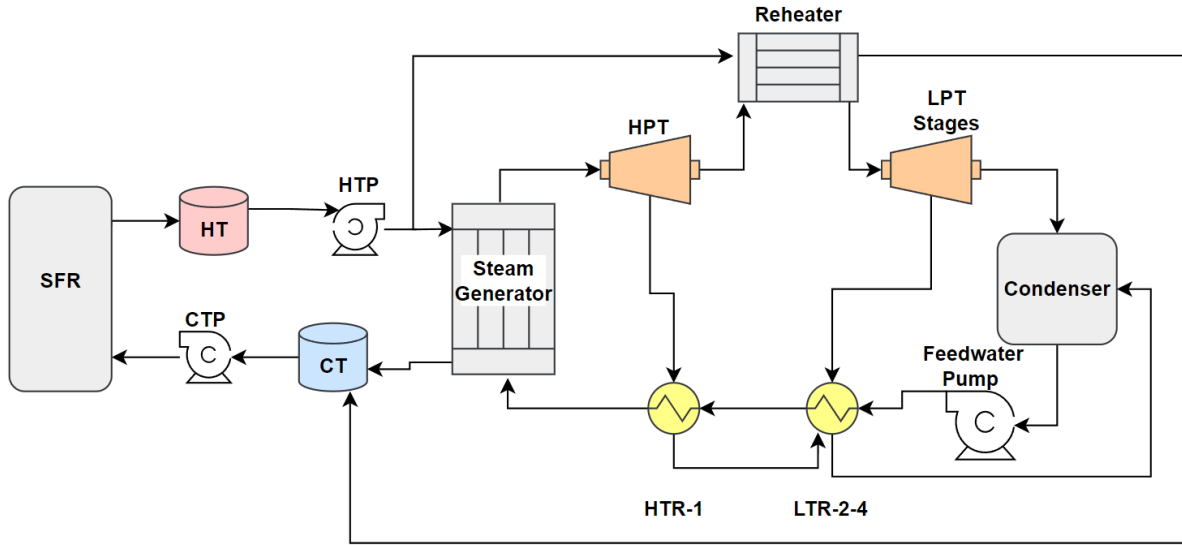
The main objective of the control system is to follow a given electricity demand profile. The control system has two actuators that change the following flow rates: 1) \dot{m} from the hot tank through the steam generator to the cold tank 2) \dot{m} of the Rankine cycle.

The flow rate of the Rankine cycle at max power is calculated in the python steady state model. The relationship between the flow rate of the Rankine cycle and power output is linear. The flow rate of steam is determined based on the desired power output. Then the flow rate of the molten salt is calculated based on the steam cycle flow rate using the following energy balance.

$$\dot{m}_{TES} c_p (T_{hot} - T_{cold}) = \dot{m}_{steam} (h_{out} - h_{in}) \quad (10)$$

Figure 3 shows a simplified model diagram with labeled components, lists the controlled quantities, governed components, reference values, and operation modes. There are three modes of operation:

1. Charging: When the demand is less than 345 MW_e
2. Boosting: When the demand is greater than 345 MW_e
3. Steady State: When the TES is full/empty the system goes to steady state operation at 345 MW_e



Controlled Quantity	Governed Component	Reference Value	Operational Mode
Electrical Output	Feedwater Pump \dot{m}	Demand	All modes
Steam Pressure HPT	HPT Partial Arc Admission	200 bar	All modes
Steam Temperature	HTP \dot{m}	varies	All modes
Level in Hot Tank	HTP \dot{m}	min/max tank level	Steady State
Salt Temperature Hot Tank	CTP \dot{m}	520 °C	All modes

FIGURE 3 Simplified model diagram. Sodium fast reactor (SFR), hot tank (HT), hot tank pump (HTP), cold tank pump (CTP), cold tank (CT), high pressure turbine (HPT), low pressure turbine (LPT) stages, high temperature regenerator (HTR), low temperature regenerator (LTR). Three LPT stages and two feedwater regenerators are not shown in this diagram.

The electrical output of the system is controlled by the mass flow rate in the feedwater pump. A model for the relationship between mass flow rate of steam, power demand, wet bulb temperature, and condensing pressure was determined using the python steady state model. The controls system takes power demand and wet bulb temperature as inputs and calculates the corresponding mass flow rate of the steam cycle to match the desired demand. The steam pressure in the HPT is controlled using partial arc admission. This is similar to throttling, however, it does not consider thermodynamic losses¹⁷. Steam temperature at the outlet of the steam generator is controlled by the mass flow rate of molten salt in the steam generator. During steady state operation, the level in both the hot and cold tank must remain constant. The mass flow rate of the HTP is set equal to the mass flow rate of the CTP. This keeps the level in each tank constant. To maintain the state points in the steam cycle during steady state operation, power is generated at the nominal level 345 MW. The salt temperature in the hot tank is controlled by the mass flow rate of cold salt through the sodium fast reactor.

3 | CASE STUDY

To demonstrate the dynamics of the model, a case study simulating scaled historical load data from the Electric Reliability Council of Texas (ERCOT) will be presented in this section. The case study is over July 1 - July 20, 2021. These dates were selected to show how intermittent renewable energy can affect the demand. The hourly production from wind, solar, and total electricity produced were obtained from the US Energy Information Administration (EIA). Figure 4 shows how renewables affect the overall energy demand to be met by power providers. When considering renewables by subtracting their contributions from the total electricity produced, the average electricity demand decreases by 19% and the range increases by 23%. This demonstrates how the unpredictable nature of renewables can create a more volatile energy profile for traditional power providers to meet. The bottom curve in Figure 4 is the demand the model will follow which is the total electricity generation over the given time frame minus the production by solar and wind. The magnitude of the demand is scaled down so the average value is near the steady state power output of a single Natrium system.

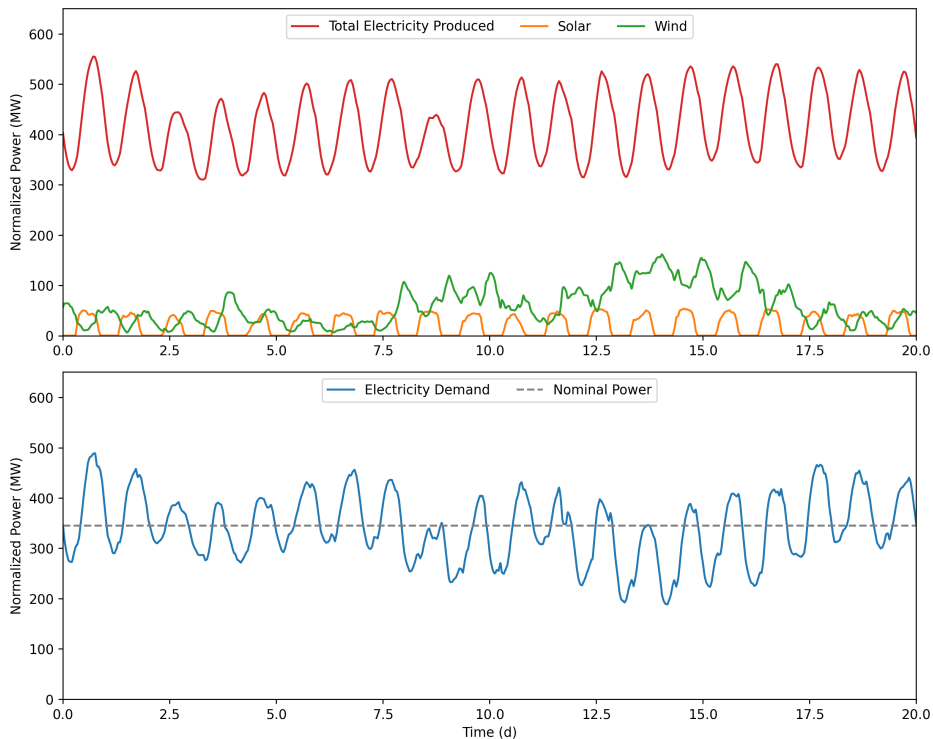


FIGURE 4 Electricity demand and renewable penetration normalized per Natrium system. Top: Total electricity produced, solar and wind production. Bottom: Total electricity demand minus renewable energy. This is the demand the system will meet.

In the first 8 days, solar and wind follow a somewhat predictable pattern, however, after day 8, there is a substantial increase in wind power. The increased wind production brings the demand the Natrium system needs to meet down. This example highlights the impact of renewable energies, such as wind and solar, on creating a more dynamic demand profile for conventional power plants to meet. The significance of thermal energy storage becomes evident as it plays a crucial role in the providing the NHES with the flexibility required to meet varying demand patterns.

Figure 5 shows the simulation results as the system response to the demand over the 20 day period and Figure 6 shows a zoomed in portion of the results through days 10-12.5. The system can follow the demand profile but is having difficulty boosting for the whole peak time, which caused some unmet demand for the current Natrium design. A larger molten salt storage will be needed according to the simulation. On the other hand, the demand decreases below the 345 MW_e through days 9-15. When the demand is below 345 MW, the system is in a state of charging as shown. When the TES is full, the system goes to steady state, which led to substantial power over-production that cannot be used or stored. This study helps identify the need of

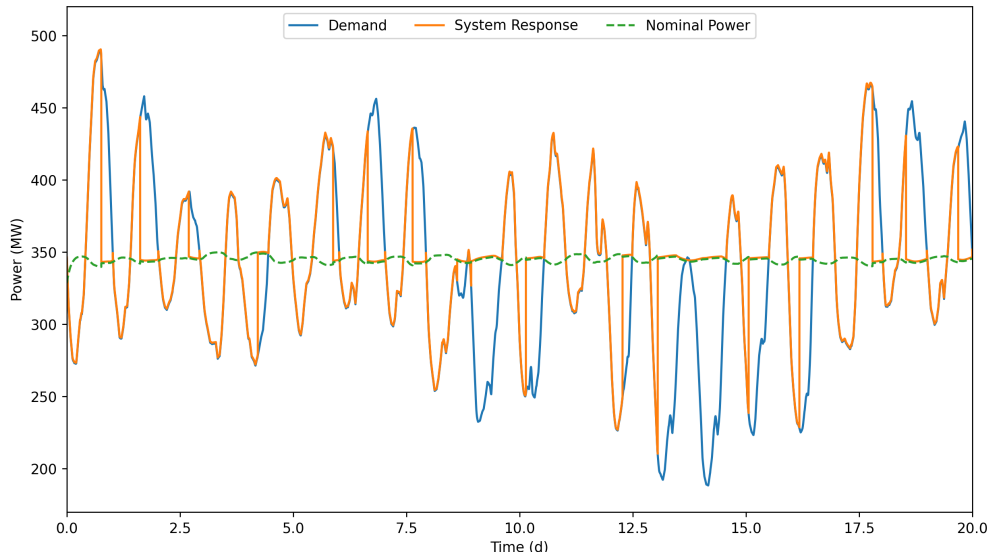


FIGURE 5 Simulation results: System response to following the demand. Nominal power of 345MWe shown.

optimization of the Natrium design for different markets. The nominal power curve has some variation due to the effects of ambient temperature affecting the thermal efficiency of the system.

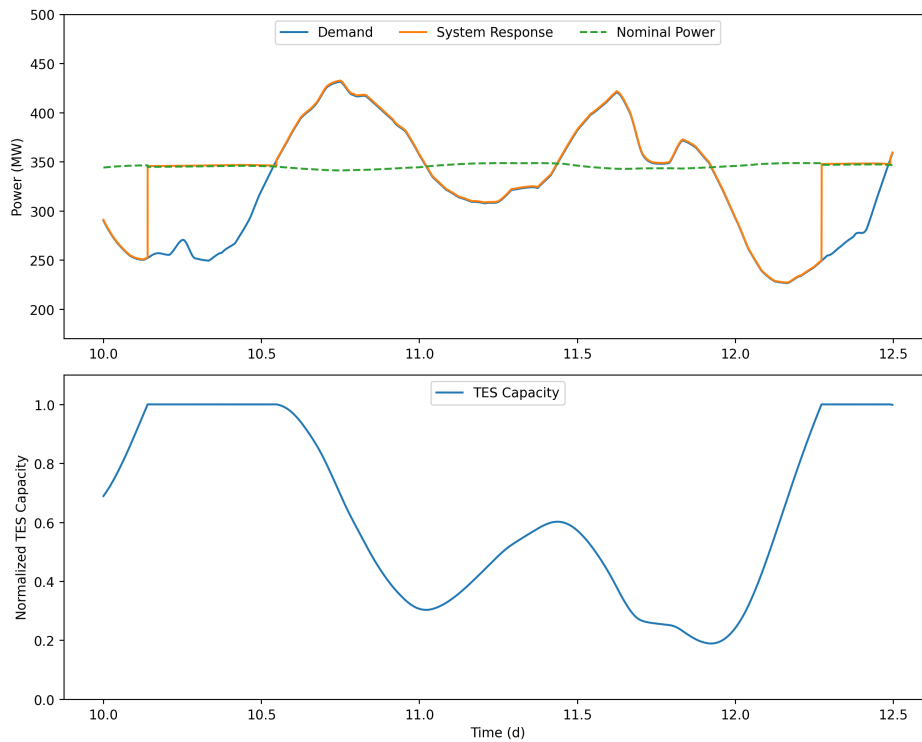


FIGURE 6 Demand, system response, and nominal power through days 10-12.5. Modes of charging, boosting and steady state on display.

Figure 7 shows the normalized TES storage capacity. This figure shows time of boosting (negative slope), charging (positive slope), and steady state (slope = 0). The bottom curve shows the mass flow rate of molten salt leaving the hot tank and the nominal power flow rate. When the mass flow rate is above nominal flow it is boosting and when it is less than nominal it is in a state of

charging. The steady state operation happens when the hot tank reaches the upper or lower limit of storage capacity. During the 20 day simulation the system boosted power output 18 times. This demonstrates the daily pattern of storage and boosting required.

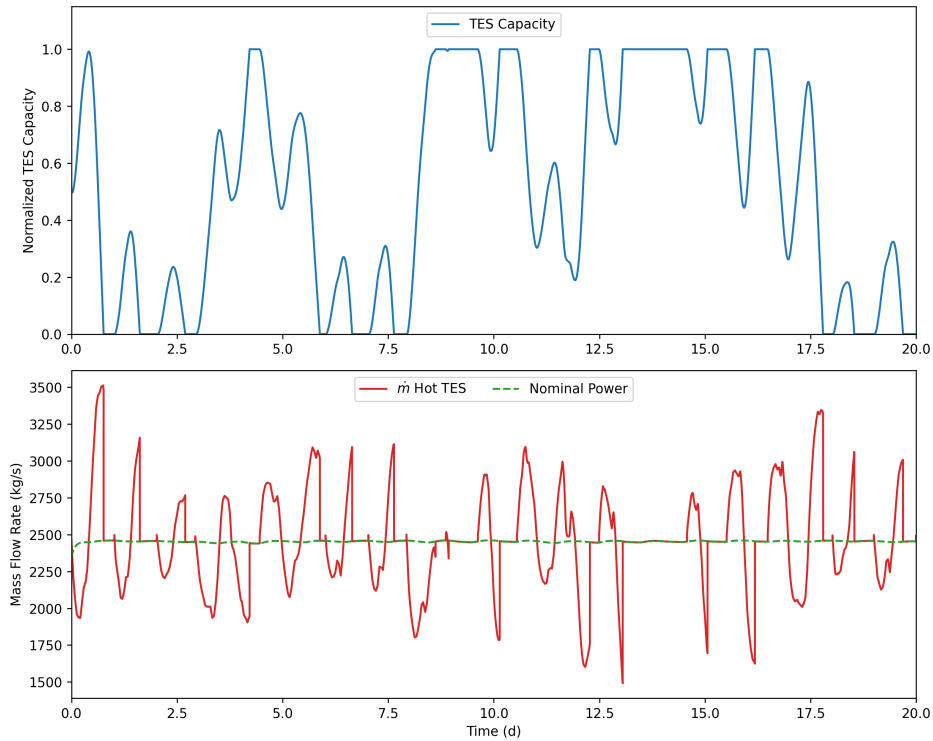


FIGURE 7 Top: Thermal energy storage hot tank level. Bottom: Mass flow rate of molten salt at hot tank outlet.

Figure 8 shows the thermal efficiency, condensing pressure, and wet bulb temperature with respect to time. The relative humidity of air affects the wet bulb temperature which further impacts the temperature of the Rankine cycle cooling water due to the evaporative cooling process often used in Rankine power cycles. Lower relative humidity/wet bulb temperatures increase the cooling ability of cooling towers and therefore lowers the condensing temperature and pressure of the steam. A lower condensing pressure will increase the thermal efficiency of the steam cycle. The average efficiency during this simulation was 44%. The ambient temperature caused the efficiency to periodically vary nearly 1% daily during the simulation.

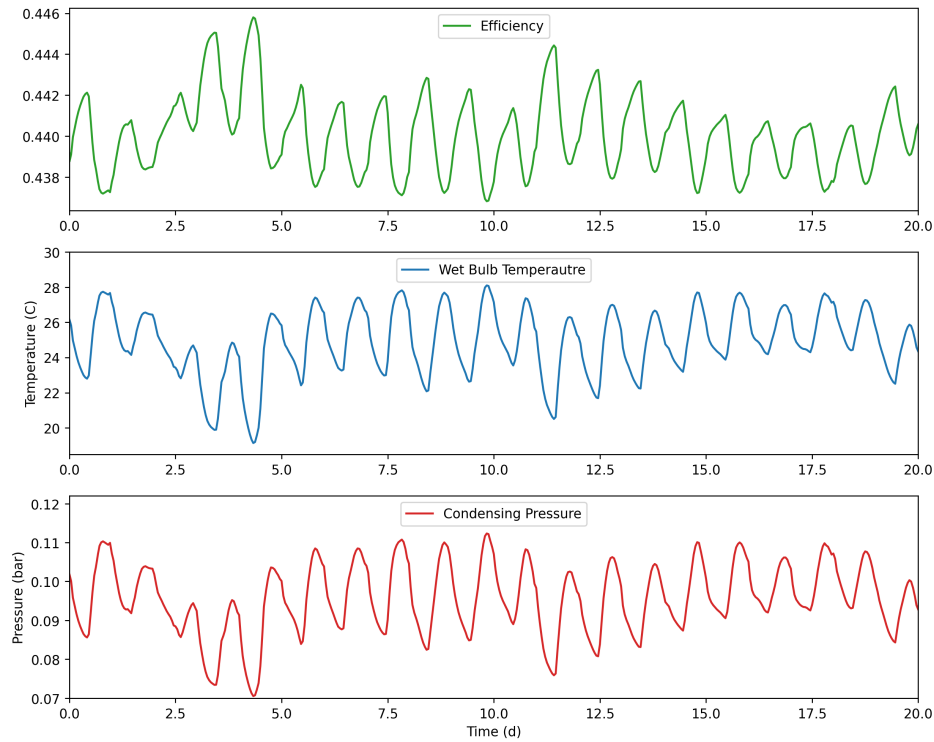


FIGURE 8 Thermal efficiency, wet bulb temperature, and condensing pressure.

4 | CONCLUSION

As a first-of-the-kind nuclear energy system, Natrium design couples a sodium fast reactor with molten salt TES. It allows for power output boosting from steady state 345 MW_e to 500 MW_e for 5.5 hours. The benefit of directly coupled energy storage is that the nuclear reactor operates at a steady state independent of the balance of plant or other industrial applications, which reduces strain on the reactor operation and increase its lifespan. This implementation of energy storage also allows for seamless integration with renewable technologies like wind and solar. Meanwhile, both the balance of plant and energy storage can be scaled for different energy markets.

In this work, a computationally efficient Dymola model of the Natrium Energy Island has been developed to analyze its performance in meeting the increasingly fluctuating demand of a specific energy market. Using ERCOT as the deregulated market for the case study, it has shown that the energy storage allows the system to store energy during low demand (off peak) periods and use it to boost power during high demand periods. This gives the Natrium system the ability to follow the load while operating the nuclear reactor (Nuclear Island) at its full capacity. For the simulation period of 20 days in July, there are time periods that the demand could not be met due to exhausted energy storage. Also, there are times that the storage is full due to low energy demand. The simulation indicates the current Natrium design could benefit from a larger energy storage for ERCOT to meet the peaks in demand. Alternatively, the Natrium system can be coupled hydrogen production, water desalination, or other industrial processes when the TES is full or the electricity price is low for price-taker models.

While the present study has provided valuable insights into a Natrium style NHES, there remains potential for further exploration and work in this area. Expanding on the groundwork established in this research, future work could include techno economic analysis of this system and a capacity optimization based on market location. This would provide insight into the economic impact of thermal energy storage on a Natrium style NHES, and identify the relationship between renewable energy production and optimal thermal energy storage size.

Declaration of Competing Interest

The authors declare that they have no known competing financial interests or personal relationships that could have appeared to influence the work reported in this paper.

Acknowledgments

The authors would like to thank the financial support from the US Department of Energy (DOE) Nuclear Energy University Program under the Award No. DE-NE0009159

REFERENCES

1. Branker K, Pathak M, Pearce J. A review of solar photovoltaic levelized cost of electricity. *Renewable and Sustainable Energy Reviews*. 2011;15(9):4470–4482. Number: 9doi: 10.1016/j.rser.2011.07.104
2. Denholm P, King JC, Kutcher CF, Wilson PP. Decarbonizing the electric sector: Combining renewable and nuclear energy using thermal storage. *Energy Policy*. 2012;44:301–311. doi: 10.1016/j.enpol.2012.01.055
3. OECD, Nuclear Energy Agency. *Technical and Economic Aspects of Load Following with Nuclear Power Plants*. Nuclear Development OECD, 2011
4. Owen AD. The economic viability of nuclear power in a fossil-fuel-rich country: Australia. *Energy Policy*. 2011;39(3):1305–1311. doi: 10.1016/j.enpol.2010.12.002
5. NEA. *Nuclear Energy Today: Second Edition*. OECD Publishing. 2012.
6. Locatelli G, Boarin S, Fiordaliso A, Ricotti ME. Load following of Small Modular Reactors (SMR) by cogeneration of hydrogen: A techno-economic analysis. *Energy*. 2018;148:494–505. Publisher: Pergamondo: 10.1016/j.energy.2018.01.041
7. Forsberg C. Hybrid systems to address seasonal mismatches between electricity production and demand in nuclear renewable electrical grids. *Energy Policy*. 2013;62:333–341. doi: 10.1016/j.enpol.2013.07.057
8. Khamis I, Koshy T, Kavvadias KC. Opportunity for Cogeneration in Nuclear Power Plants. In: 2013.
9. Mikkelsen D, Frick K. Analysis of controls for integrated energy storage system in energy arbitrage configuration with concrete thermal energy storage. *Applied Energy*. 2022;313:118800. doi: 10.1016/j.apenergy.2022.118800
10. Esteves OLA, Gabbar HA. Scopus - Document details - Nuclear-Renewable Hybrid Energy System with Load Following for Fast Charging Stations. *Energies*. 2023. doi: 10.3390/en16104151
11. Bryan J, Meeke A, Dana S, Islam Sakir MS, Wang H. Modeling and design optimization of carbon-free hybrid energy systems with thermal and hydrogen storage. *International Journal of Hydrogen Energy*. 2023. doi: 10.1016/j.ijhydene.2023.03.135
12. Garcia HE, Chen J, Kim JS, et al. Dynamic performance analysis of two regional Nuclear Hybrid Energy Systems. *Energy*. 2016;107:234–258. doi: 10.1016/j.energy.2016.03.128

13. Wodrich L, H. LAJ, Kozlowski T, Brooks CS. Modeling of an Energy-Diverse Embedded Grid for Microreactor Integration. *Nuclear Technology*. 2023. ISSN: 0029-5450.
14. Binder W, Paredis C, Garcia H. Hybrid Energy System Modeling in Modelica. In: 2014:979–988
15. Saeed R, Shigrekar A, Mikkelsen D, et al. Multilevel Analysis, Design, and Modeling of Coupling Advanced Nuclear Reactors and Thermal Energy Storage in an Integrated Energy System. Tech. Rep. INL/RPT-22-69214-Rev000, 1890160, 2022
16. Frick KL, Alfonsi A, Rabiti C, Mikkelsen DM. Hybrid User Manual.
17. Greenwood M. TRANSFORM - TRANsient Simulation Framework of Reconfigurable Models. 2017. Language: en
18. Elsheikh A, Widl E, Palensky P. Simulating complex energy systems with Modelica: A primary evaluation. In: 2012:1–6. ISSN: 2150-4946
19. Dymola - Dassault Systèmes®. <https://www.dymola.com>.
20. Sodium. <https://sodiumpower.com>.
21. Reddy Prasad D, Senthilkumar R, Lakshmanarao G, Krishnan S, Prasad N. A critical review on thermal energy storage materials and systems for solar applications. *AIMS Energy*. 2019;7(4):507–526. doi: 10.3934/energy.2019.4.507
22. Meek A, Dana S, Basnet M. Steady State Modeling of a Regenerative Rankine Cycle for the Sodium System. In: 2023.
23. Wu Yt, Li Y, Lu Yw, Wang Hf, Ma Cf. Novel low melting point binary nitrates for thermal energy storage applications. *Solar Energy Materials and Solar Cells*. 2017;164:114–121. doi: 10.1016/j.solmat.2017.02.021
24. ZAVOICO AB. Solar Power Tower Design Basis Document, Revision 0. tech. rep., 2001. doi:10.2172/786629.



APPENDIX

A PINCH POINT PLOTS

The heat exchangers use a modified effectiveness equation to calculate the heat transfer but don't ensure the second law of thermodynamics is conserved. Temperature profile plots show that the second law of thermodynamics is kept in the steam generator and reheat heat exchangers.

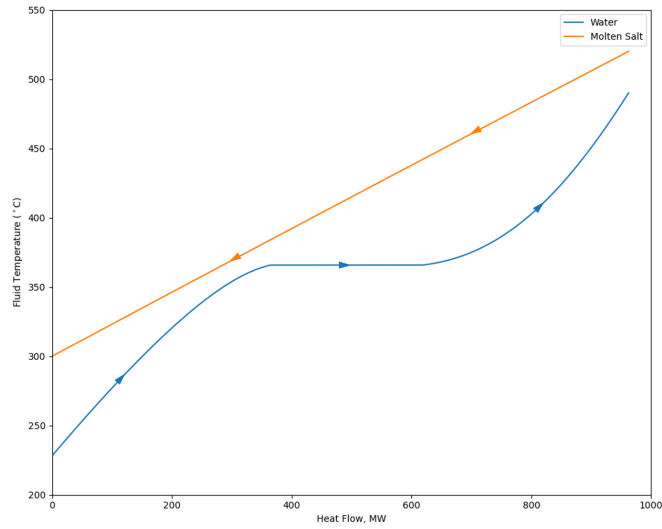


FIGURE A1 Steam generator temperature profile.

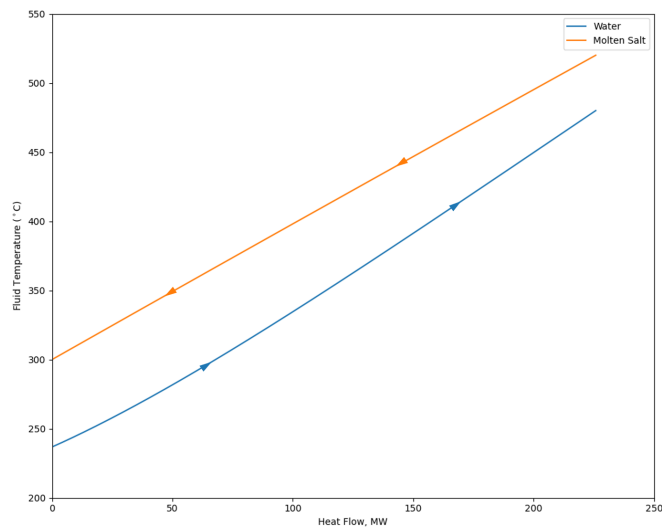


FIGURE A2 Reheater temperature profile.

B MOLTEN NITRATE SALT PROPERTIES

TABLE B1 Properties of molten nitrate salt (60% NaNO₃ and 40% KNO₃)^{23,24}.

Property	Solar Salt
Melting Point ($^{\circ}C$)	220
Boiling Point ($^{\circ}C$)	565
Thermal Conductivity (W/mK)	0.53
Density (kg/m^3)	1804
Specific Heat Capacity (kJ/kgK)	1.52
Dynamic Viscosity ($Pa\ s$)	0.00169
Prandtl Number	4.85
Cost ($\$/kWh$)	5.8

C MODIFIED RANKINE CYCLE STATE POINTS

TABLE C2 Input parameters in the Dymola model.

Parameter	Value	Description
Q_{in}	833.69 MW	Thermal power of nuclear reactor
Area	1460 m ²	Cross sectional area of TES tanks
H	7 m	Height of TES available
$P_{turbinein}$	200 bar	Inlet pressure to turbine
T_{steam}	490 °C	Inlet temperature of steam to turbine
$T_{hottank}$	520 °C	Hot tank storage temperature
$T_{coldtank}$	300 °C	Cold tank storage temperature
ϵ_{regen}	0.90	Effectiveness of the regenerators
$\epsilon_{steamgen}$	0.96	Effectiveness of the Steam Generator

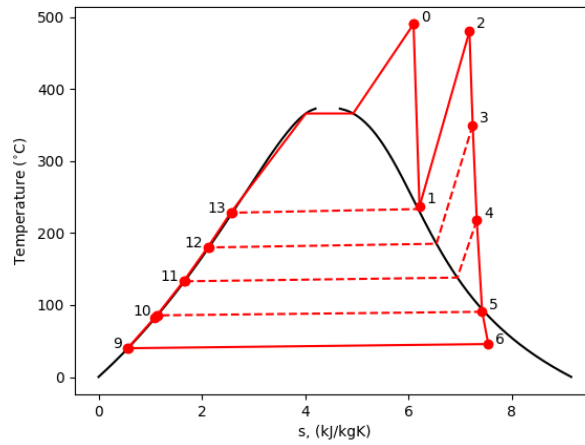


FIGURE C3 T-s diagram of the Rankine power cycle.

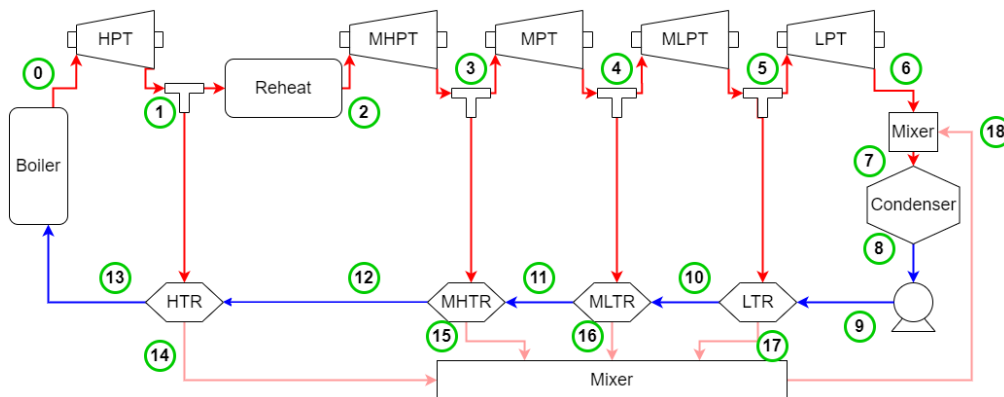


FIGURE C4 State points of the steam cycle.